ACS OMEGA

Open Access

http://pubs.acs.org/journal/acsodf

Article

Development of Active Antibacterial CEO/CS@PLA Nonwovens and the Application on Food Preservation

Hui Sun, Bingbing Wang, Youxiu Xie, Fengchun Li, Tao Xu, and Bin Yu*

Cite This: *ACS Omega* 2023, 8, 42907−42920

Read Online

ACCESS | Metrics & More | Article Recommendations

ABSTRACT: The biodegradable activity antibacterial materials have been widely applied on food preservation because they not only protect foods from pathogenic attacks but also relieve environmental pollution. Biodegradable melt-blown nonwovens (MB) have several advantages over the other materials in terms of a simpler and more environmentally friendly fabrication process, higher specific surface area, and lower cost. Herein, polylactic acid (PLA) MB is first modified by polydopamine (PDA) to activate the surface. Then, chitosan (CS) and cinnamon essential oil (CEO) are used to decorate the surface of the modified PLA MB via a simple one-pot method to prepare CEO/CS@PLA MB with different CEO contents. Compared with PLA MB, CEO/CS@PLA MB had a rougher surface and larger average fiber diameter, while the average pore diameter and air permeability reduced. The input of CEO led to a decrease in the tensile strength of CEO/CS@PLA MB and an obvious increase in the elongation at break. The combination of CS and CEO shows excellent synergistic antibacterial effect. The antibacterial efficiencies of CEO/CS@PLA MB against *Escherichia coli* and *Staphylococcus aureus* enhance with the increase of the CEO content. When the weight ratio of CS to CEO is 1:2, the antibacterial efficiencies of CEO_2/CS@PLA MB against *E. coli* and *S. aureus* are 99.98 and 99.99%, respectively. When being applied to the preservation of fresh strawberry, CEO_2/CS@PLA MB can effectively inhibit the microbial growth in strawberry and reduce decay, which extends the shelf time of strawberry.

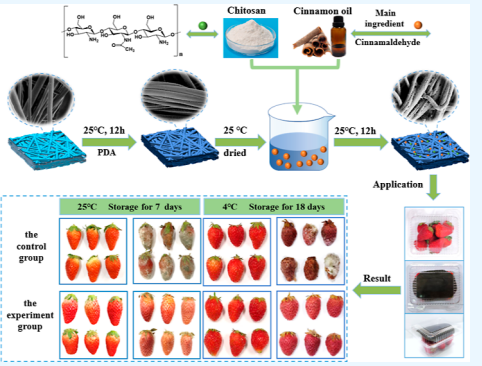

INTRODUCTION

Fresh foods provide energy and nutrition for human survival and healthy but are the ideal environment for the growth of foodborne pathogens. Especially, small-sized fruits, like strawberry, are highly perishable mainly because of their intense metabolic activity, fast respiratory rate, and susceptibility to pathogenic attacks.[1] Foodborne diseases varying from mild discomfort to deadlines constitute a threat to public health. Meanwhile, food spoilage would deteriorate the problem of inadequate food supply.[2] According to the statistics of the Food and Agriculture Organization of the United Nations (FAO), about 40−50% of fruits and vegetables are consumed by microbial corrosion and the effects of oxygen and enzymes each year.[3] With the increasing concerns about the quality and safety of food and the crisis of food resources, the requirement of food preservation for fresh and safe produce is continuously promoted. The development of active antibacterial materials is simple and effective strategy to protect foods from pathogenic attacks and maintain quality.[4]

The biodegradable antibacterial materials have attracted widespread attention in food preservation. They can not only effectively extend the shelf life of food but also relieve the environmental impact of human activity.[5−7] Most of these materials consist of biodegradable polymers combined with natural or synthetic antibacterial agent. The biodegradable polymers commonly include polysaccharide,[8,9] protein,[10,11] the aliphatic polyester,[12,13] and so on. Polylactic acid (PLA), a common biodegradable aliphatic polyester, derives from renewable resources, such as corn, cassava, and sugar beet, and eventually degrades into water and carbon dioxide. PLA has been classified as Generally Recognized As Safe (GRAS) by the United States Food and Drug Administration (FDA) and used for all food packaging applications in virtue of nontoxic, nonirritating, good biocompatibility, biodegradability, and processability.[14,15]

Commonly, the active antibacterial materials for food preservation or package are made into film products.[16,17] However, film products have a complex preparation process and high cost. Recently, some new textile materials, like electrospun nonwovens, have aroused great interest of researchers on the development of active antibacterial

Received: August 15, 2023
Revised: September 21, 2023
Accepted: October 10, 2023
Published: November 2, 2023

materials for food preservation.[16,18−20] Electrospun nonwovens have an advantage of easy operation and function and low cost.[16] The ultrafine fibrous and porous structure endow electrospun nonwovens high specific surface area, which can provide more opportunities to response to changes in temperature and relative humidity of the surrounding environment and is helpful for triggering the release of active antibacterial substance.[21] Additionally, the randomly distributed and interlacing nanofibers avoid aeolotropism of electrospun nonwovens. However, the use of organic solvents is often unavoidable during the electrospinning process because polymer raw materials have to be dissolved to obtain the spinning dope. The volatilization of the organic solvent in the fiber forming stage should lead to environmentally unfriendly production condition. On the other hand, a high voltage field is indispensable to fulfill the stretchability of the injected spinning fluid, which requires rigorous ambient humidity and temperature in the whole spinning process. Compared with electrospun nonwovens, melt-blown nonwovens (MB) also has the similar randomly distributed fibrous structure to electrospun nonwovens, high specific surface area and porosity.[22] However, polymer resin just needs to be melted, and micrometer fibers are formed by the blowing of high-speed hot airflow during the fabrication of MB. Therefore, MB has milder and more environmentally friendly fabrication processes, lower cost, as well as higher mechanical property. According to our knowledge, little information on the development of MB with antibacterial activity for food preservation is available.

The antibacterial agents play a crucial role in active antibacterial materials. The active antibacterial agents can touch and migrate to the food, which can extend the shelf time of food.[23,24] Chitosan (CS) is an abundant amino-containing polysaccharide and obtained from partially deacetylated chitin.[25] Many research demonstrated that CS can inhibit the growth of variety of bacteria, fungi, and viruses due to the presence of the protonated amino groups.[26] Thus, CS has widely applied on antibacterial active food package and preservation.[27,28] For example, Ruan et al.[28] synthesized a new antibacterial CS−quaternary phosphonium salt (QP)−salicylic acid (SA) coating films by grafting QA and SA onto CS for mango preservation. Compared with mango in the control group, weight loss of mango treated by CS−QP−SA films decreased from 19.98 to 12.68%, and the decay rates reached the lowest. They thought that CS−QP−SA films effectively extended the storage time of mango. Chen et al.[29] combined the extract and CS from American cockroach to produce a new environment-friendly CS film for the package of chicken breasts and pork fats. The antioxidant activity of the CS film added American cockroach extract was 50 times higher than that of pure CS film when considering reducing capacity. This film efficiently inhibited the growth of bacteria and oxidation of the packaged food. Alshallash et al.[30] prepared a CS nanoparticle by using high-energy ball milling. Then, the CS nanoparticle is dissolved and coated on the surface of Valencia oranges in the various concentrations. They found that the treatment of the nano-CS solution with a concentration of 0.8% showed the best effects and had the lowest rate of fruit weight loss. Furthermore, the 0.8% nano-CS solution revealed the highest levels of fruit hardness and fruit pulp firmness. However, CS merely displays its antibacterial activity in an acidic medium, its antibacterial effect is limited at neutral and alkaline pH due to the poor solubility in water.[28,31,32] Additionally, CS also shows weak antibacterial activity against *Escherichia coli* and other bacteria and the sharp decrease of antibacterial property after film formation.[33]

In the last decades, people's awareness of health and food safety has been aroused. There are the growing studies focusing on the utilization of plant essential oils in consideration of the unsafety of synthetic antibacterial agent.[34] Plant essential oil are extracted from different parts of plants and a combination of various volatile lipophilic ingredients including terpenoids, glycosides, flavonoids, and polyphenols, which has been known as GRAS and safe for consumption.[35,36] Cinnamon essential oil (CEO) is one of the most effective plant essential oils against common food-borne pathogens and has excellent antioxidant property. These advantages are primarily related to cinnamaldehyde (CIN) with the content of approximately >50% in CEO, eugenol, and cinnamic acid.[37] So far, CEO has been concerned as promising substitutes for synthetic antibacterial agents.[38]

In this paper, we attempt to develop a biodegradable PLA MB with antibacterial activity for food preservation. In consideration of the inadequate antibacterial property of CS and the volatility of CEO, the combination of CS and CEO was used to decorate the surface of the modified PLA MB by polydopamine (PDA) via a simple one spot method. Then, the obtained CEO/CS@PLA MB was applied on the practical preservation of perishable strawberries, and the influence of this antibacterial material on the shelf time of fresh strawberry was evaluated. We hope that our studies may diversify antibacterial active materials for food preservation.

EXPERIMENTAL SECTION

Materials. PLA MB was purchased from Quanzhou Smartwin import trade Co., Ltd. It has an areal density of 40 g/m^2 and the thickness of 0.24 ± 0.01 mm. CS with the deacetylation degree over 95% and viscosity of 100−200 MPa·s, dopamine hydrochloride with a purity of 98%, and tris(hydroxymethyl)methyl aminomethane with a purity of over 99.5% were purchased from Shanghai Aladdin Biochemical Technology Co., Ltd. CEO including a CIN content of more than 85% was bought from Jiangxi Yixin Spice Co., Ltd. Glacial acetic acid, hydrochloric acid (HCl) and ethyl alcohol were obtained from Hangzhou Gaojing Fine Chemical Co., Ltd. Tween-80 with a hydrophilic−lipophilic balance of 16.7, phenolphthalein, and 1,1-diphenyl-2-trinitrophenylhydrazine (DPPH) with a purity of 96% were bought from Shanghai Maclin Biochemical Technology Co., Ltd. *E. coli* [CMCC(B) 44102] and *Staphylococcus aureus* [CMCC(B) 26003] were obtained from Beijing Baocang Biotechnology Co., Ltd. Yeast extract powder, peptone, and nutrient agar medium were purchased from Hangzhou Best Biotechnology Co., Ltd. Normal saline was purchased from Sichuan Kelun Pharmaceutical Co., Ltd. Deionized water was prepared in our laboratory. All of the chemicals are unpurified.

Hydrophilic Modification of PLA MB. Prior to the experiment, PLA MB was scissored into a square with 10 × 10 cm^2, washed by ethyl alcohol, and dried at 40 °C in vacuum oven. 0.48 g of tris(hydroxymethyl)methyl aminomethane was added into 400 mL of deionized water and stirred until being sufficiently dissolved. HCl with a concentration 0.1 mol/L was cautiously added into the

https://doi.org/10.1021/acsomega.3c06024
ACS Omega 2023, 8, 42907−42920

Scheme 1. Preparation Route of CEO/CS@PLA MB

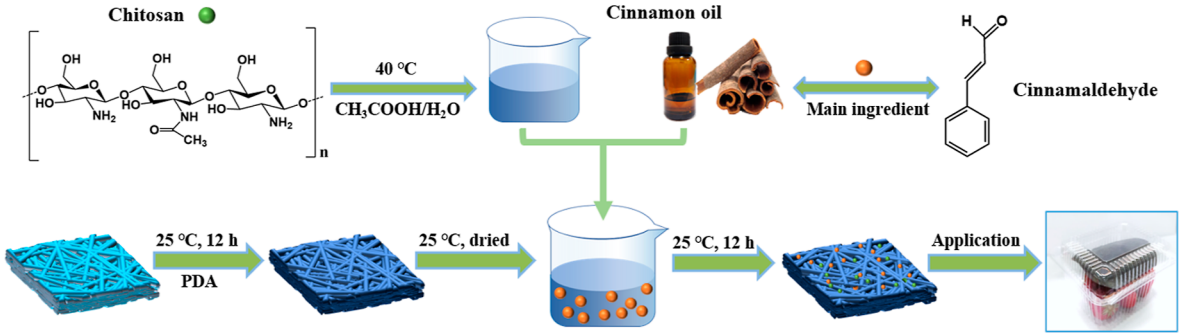

above solution and used on the adjustment of the pH of the solution to 7.5−8 to obtain Tri-HCl buffer solution. Then, dopamine (DA) was dissolved into the Tri-HCl buffer solution in the concentration of 1.25 mg/mL. Next, the pretreated PLA MB was put into the DA solution and slowly stirred at 25 °C for 12 h. Finally, the modified PLA MB by PDA was taken out and alternately washed by ethyl alcohol and deionized water multiple times. After that time, the modified PLA MB was dried at 25 °C in the atmosphere.

Preparation of CEO/CS@PLA MB. 1.01 g of CS was added into 100 g of acetic acid aqueous solution with a volume concentration of 1% and stirred at 40 °C until being dissolved. Tween-80 was mixed with the above solution, and the mixture was stirred at room temperature for 2 h. Then, CEO with different weights was dropped in the CS solution with a certain weight to form the mixed CEO/CS solution with different weight ratios. The weight ratios of CS and CEO in the solution are 1:0, 1:0.5, 1:1, 1:1.5, and 1:2, respectively. Next, the modified PLA MB was put into the above CEO/CS solution and stirred at 25 °C for 12 h. After the reaction was finished vis the simple one-pot method, the obtained CEO/CS@PLA MB was washed by ethyl alcohol and deionized water in turn and then dried at 40 °C in vacuum oven. CEO/CS@PLA MB with the weight ratios of CS to CEO of 1:0, 1:0.5, 1:1, 1:1.5, and 1:2 are marked by CS@PLA MB, $CEO_{0.5}$/CS@PLA MB, CEO_1/CS@PLA MB, $CEO_{1.5}$/CS@PLA MB, and CEO_2/CS@PLA MB, respectively. The preparation route of CEO/CS@PLA MB is shown in Scheme 1.

Methods. *SEM.* The morphologies of the samples were observed by a Vltra55 field emission scanning electron microscope (SEM, Carl Zeiss Corporation). The samples were cut into small pieces and fixed on the copper sample stage by the use of the conductive tape. All of the samples were plated with a thin layer of gold before inspection. The acceleration voltage was 3 kV.

Average Pore Diameter. The average pore diameter measurement of the samples was carried out by a TOPAS PSM-165 pore diameter tester (TOPAS Corporation) according to the bubble method and repeated three times.

Air Permeability. The air permeability of the samples was tested by a YG461E air permeability tester (Fangyuan Instrument Co., LTD) at room temperature. The diameter of the samples was 13 cm, and the testing pressure was 200 Pa. Each sample was tested five times.

Infrared Spectroscopy. Attenuated total reflection Fourier transform infrared spectroscopy (ATR−FTIR) was carried out on a Nicolet 57000 spectrometer (Thermo Scientific Corporation) in the spectral range 4000−500 cm^{-1}. Each sample was scanned 32 times.

Loading Ratio. The reaction of CEO/CS solution with the modified PLA MB was quantificationally expressed by the loading ratio, as shown in the following eq 1.

$$\text{the loading ratio } (\%) = \frac{m_l - m_p}{m_p} \times 100 \quad (1)$$

where m_l is the weight of CEO/CS@PLA MB and m_p is the weight of the modified PLA MB. Three samples with the same content of CEO were repeatedly tested, and the average value was obtained.

X-ray Diffraction. The X-ray diffraction (XRD) pattern was recorded using a D8 discover X-ray diffractometer (Bruker AXS Corporation) with Cu Kα irradiation at 40 kV and a step of 5°/min in the diffraction angle (2θ) range of 10−40°.

Water Contact Angle. Water contact angle (WCA) of the samples was measured by a JY-82B Video contact angle tester (Dingsheng testing machine testing equipment Co., LTD). The samples were scissored into the pieces with 1 × 1 cm^2 and sticked on the glass slide. WCA was obtained after 4 μL per drop of deionized water was deposited onto the surfaces of the samples. Three different surface regions of each sample were measured. The image of the deionized water drop was captured with a camera.

Mechanical Property. The tensile properties of the samples were tested by an Instron-3369 universal testing machine (Instron corporation). The samples were longitudinally cut into the bars with 50 × 20 mm^2 and placed at room temperature in the atmosphere for 48 h before measurement. The effective testing distance was 20 mm, and the tensile speed was 50 mm/min. The tensile test was repeated five times for each sample.

Antibacterial Activity. The antibacterial activity of the samples against both Gram-negative *E. coli* and Gram-positive *S. aureus* was evaluated by the oscillation method. All the required glassware and other handling materials were sterilized before use under standard conditions. 100 μL of nutrient broth containing bacteria was added to 900 μL of buffered saline and was placed at 37 °C for 24 h to obtain a saturated bacterial suspension of about 108 cfu/mL. 100 μL of the saturated bacterial suspension was added into 900 μL of buffered saline and diluted 10^4 times with deionized water. Then, 0.01 g of the sample was immersed in 1 mL of the diluted bacterial suspension and incubated with shaking in a constant temperature water bath shaker at 37 °C for 24 h. 10 μL of the diluted solution was poured out, evenly coated the

https://doi.org/10.1021/acsomega.3c06024
ACS Omega 2023, 8, 42907−42920

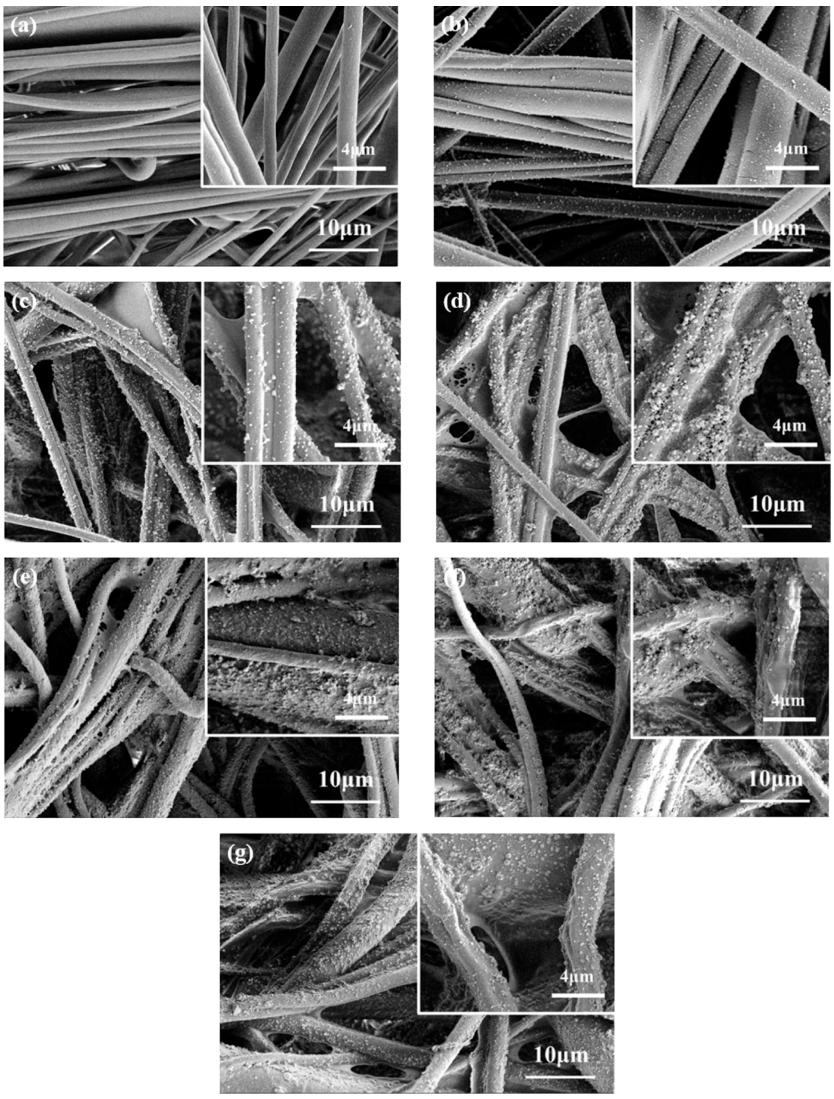

Figure 1. SEM images of PLA MB, the modified PLA MB, CS@PLA MB, and CEO/CS@PLA MB with different CEO contents: (a) PLA MB, (b) the modified PLA MB, (c) CS@PLA MB, (d) $CEO_{0.5}$/CS@PLA MB, (e) CEO_1/CS@PLA MB, (f) $CEO_{1.5}$/CS@PLA MB, and (g) CEO_2/CS@PLA MB.

agar plate, and incubated with shaking at 37 °C for 24 h. The number of living bacteria on the agar plates was counted. Each sample was repeatedly tested three times. The pure bacterial suspension was selected as a control. The antibacterial efficiency of the samples was calculated using eq 2.

$$\text{the antibacterial efficiency } (\%) = \frac{A_0 - A}{A_0} \times 100 \quad (2)$$

where A_0 is the number of bacteria colonies of the control sample and A is the number of bacteria colonies of the corresponding samples.

Application. Fresh strawberries were bought from the local supermarket, and similar ripeness and size were picked. All strawberries were randomly divided into three groups, that is, the control group, the comparative group, and the experimental group. Each group includes 27 strawberries with a weight of 195 ± 10 g. Then, 27 strawberries were randomly and equally divided into three polyester boxes of 0.25 L with a lid and without hole. The strawberries in the control group were packed in the polyester box. In the comparative group, the strawberries in the box were covered PLA MB with a roughly similar size to the bottom area of the box, while the strawberries in the experiment group were covered by CEO_2/CS @PLA MB with the same size as PLA MB. Three groups of strawberries were stored in a 60 ± 5% humidity environment at 4 ± 1 and 25 ± 3 °C, respectively.

Appearance. In three groups of strawberries stored at 4 ± 1 and 25 ± 3 °C, two strawberries per box were randomly selected and photographed on each sampling day, respectively.

Weight Loss. To measure the weight loss of strawberries, each sample per box was weighed on the day they were purchased (the zeroth day) and each sampling day at room temperature, respectively. The weight loss was expressed as the percentage of the primary weight according to eq 3.[39]

$$\text{weight loss } (\%) = \frac{m_0 - m_t}{m_0} \times 100 \quad (3)$$

where m_0 is the initial weight of strawberries and m_t is the final weight at the sampling day.

https://doi.org/10.1021/acsomega.3c06024
ACS Omega 2023, 8, 42907−42920

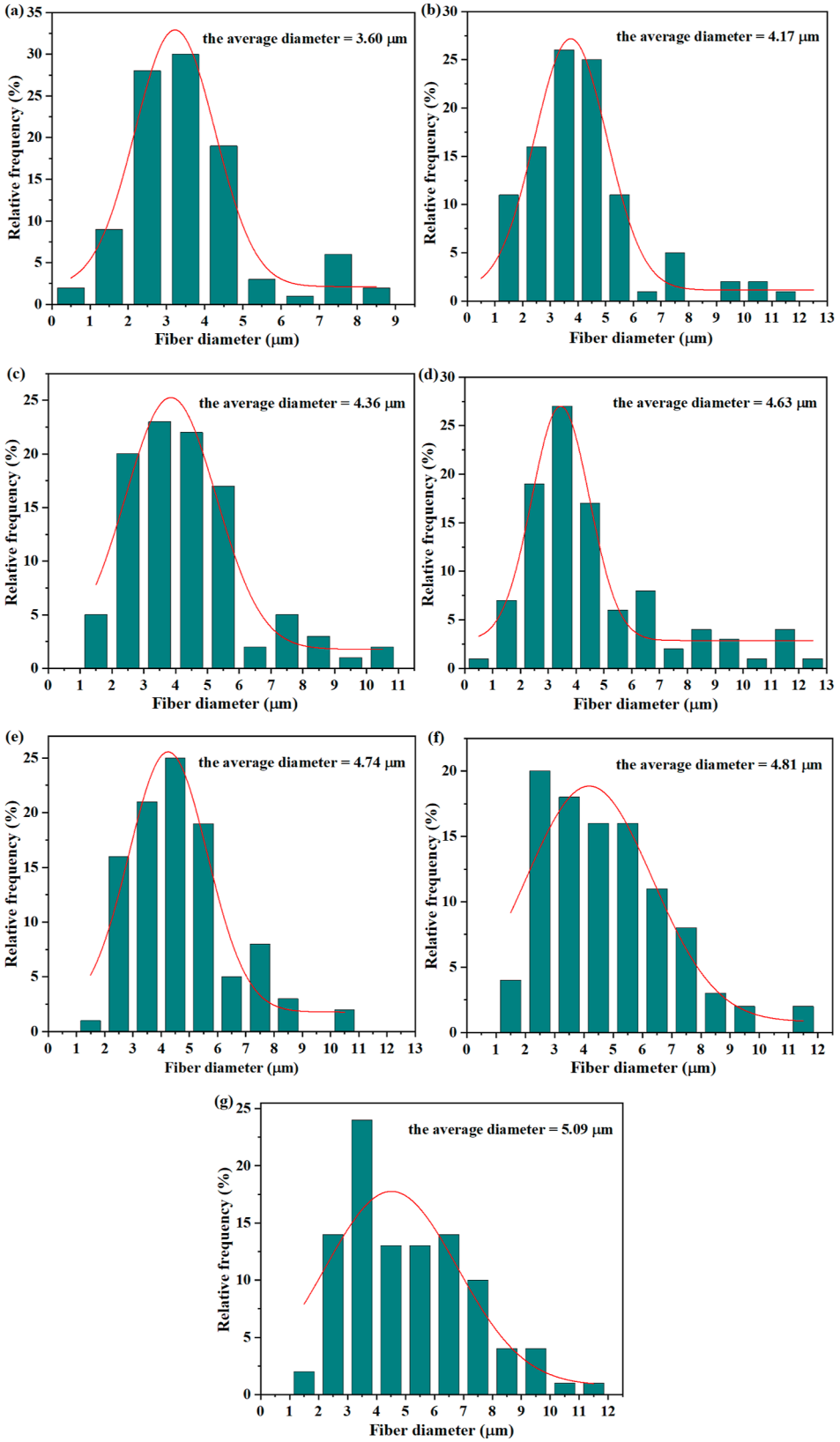

Figure 2. Fiber diameter distribution and average diameter of PLA MB, the modified PLA MB, CS@PLA MB, and CEO/CS@PLA MB with different CEO contents: (a) PLA MB, (b) the modified PLA MB, (c) CS@PLA MB, (d) $CEO_{0.5}$/CS@PLA MB, (e) CEO_1/CS@PLA MB, (f) $CEO_{1.5}$/CS@PLA MB, and (g) CEO_2/CS@PLA MB.

Decay Incidence. According to the method described by Zheng et al.,[40] the severity of strawberries decay was observed and evaluated using a scale where 0 = no signs of decay, 1 = 1−10% decay, 2 = 11−25% decay, 3 = 26−40% decay, 4 = 41−50% decay, and 5 = >51% decay. The decay incidence was calculated using eq 4.

https://doi.org/10.1021/acsomega.3c06024
ACS Omega 2023, 8, 42907−42920

$$\text{Decay incidence (\%)} = 100 \times \left(\sum (\text{decay level}) \times (\text{number of fruit at the decay level})\right) / (\text{total number of fruit in the treatment} \times \text{the highest score}) \quad (4)$$

DPPH Radical Scavenging Activity. The antioxidant activity of strawberries was evaluated based on the DPPH radical scavenging capacity method.[41] 3 mL of ethyl alcohol DPPH solution (0.1 mM) was mixed with 1 mL of strawberry juice or distilled water (as the control). Then, the solutions were kept in the dark for 30 min. The absorbance of the supernatant was tested by an Agilent Cary-60 ultraviolet (UV)-visible light (VIS) spectrophotometer (Agilent Technology Co. LTD) and read at 517 nm. The results were expressed as the inhibition percentage of the DPPH radical and calculated using eq 5.

$$\text{DPPH radical scavenging activity (\%)} = [(A_c - A_s)/A_c] \times 100 \quad (5)$$

where A_s is the absorbance of sample and A_c is the absorbance of control.

Titratable Acidity. Strawberries were juiced by using a homogenizer, and 10 mL of the obtained strawberry juice was uniformly mixed with 100 mL of deionized water and filtered. Then, 10 mL of filtered liquid was titrated by NaOH (0.1 M) with phenolphthalein serving as the indicator. The titratable acidity (TA) was calculated by using eq 6.[42]

$$\text{TA (\%)} = [(V_1 \times 0.1 \times 0.064 \times V_0)/(m \times V_2)] \times 100 \quad (6)$$

where V_1 is the volume of NaOH used for titration, 0.1 is the molarity of NaOH solution, 0.064 is the conversion factor for citric acid, V_0 is the total volume of strawberry juice, V_2 is the volume of strawberry juice for titration, and m is the total weight of strawberries.

RESULTS AND DISCUSSION

SEM Analysis. Figure 1 shows SEM images of PLA MB, the modified PLA MB, and CEO/CS@PLA MB with different CEO contents. The fiber surface of PLA MB is smooth (Figure 1a). The fibers are randomly arranged and interweaved, resulting in the inherent high porosity of PLA MB. Due to the hydrophobicity and lack of active functional groups of PLA, PDA is polymerized on the surface of PLA MB. The modification of PDA can bring in some active hydrophilic group, like hydroxy groups (−OH) and amino ($-NH_2$), on the surface of PLA MB, which is beneficial to the subsequent surface decoration.[43,44] After hydrophilic modification, a uniform and compact PDA layer is formed on the surface PLA fibers vis the oxidative polymerization of monomer DA. Some small granular PDA aggregates appear on the fiber surface (Figure 1b). The surface of the CS@PLA MB becomes rougher because some small CS particles appear on the PLA fiber surface (Figure 1c). Meanwhile, the partial fibers are adhered by the thin film, suggesting that CS has the good film-forming characteristics.[34] When the combination of CS and CEO is loaded onto the surface of the modified PLA MB, more small particles appear on the surface of PLA fibers, and the roughness of the surface of CEO/CS@PLA MB further increases with the increasing of the CEO content (Figure 1d−g).

The fiber diameter distribution and average diameter of PLA MB, the modified PLA MB, CS@PLA MB, and CEO/CS@PLA MB with different CEO contents are obtained by the Image software analysis of Figure 1 and plotted in Figure 2. The fiber diameter distribution of PLA MB is in the range from 0.50 to 8.50 μm, and the average diameter of PLA fibers is about 3.60 μm (Figure 2a). After being modified by PDA and the following loading of CS, the fiber diameter distribution of the modified PLA MB and CS@PLA MB becomes broad, and the average diameter increases (Figure 2b,c). For CEO/CS@ PLA MB, with the increasing CEO content, the fiber diameter distribution and average diameter constantly enhance (Figure 2d−g), which is attributed to the rougher surface of PLA fibers and the adhesion between the fibers, as observed in SEM analysis.

Average Pore Diameter and Air Permeability. The average pore diameter and air permeability of PLA MB, the modified PLA MB, CS@PLA MB, and CEO/CS@PLA MB with different CEO contents are shown in Figure 3. The

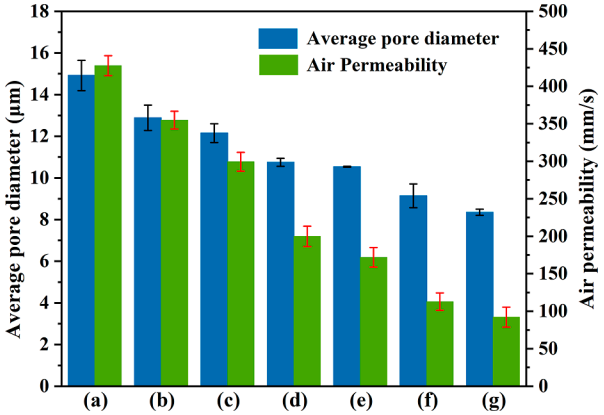

Figure 3. Average pore diameter and air permeability of PLA MB, the modified PLA MB, CS@PLA MB, and CEO/CS@PLA MB with different CEO contents: (a) PLA MB, (b) the modified PLA MB, (c) CS@PLA MB, (d) $CEO_{0.5}$/CS@PLA MB, (e) CEO_1/CS@PLA MB, (f) $CEO_{1.5}$/CS@PLA MB, and (g) CEO_2/CS@PLA MB.

average pore diameter of PLA MB is 14.92 μm, and the air permeability is 427.64 mm/s. After the hydrophilic modification and coating of CS, the average pore diameter and air permeability of the modified PLA MB and CS@PLA MB reduce. The reason is the film formation of PDA and CS in sequence on the surface of PLA fibers and the adhesion between fibers. The average pore diameter and air permeability of CEO/CS@PLA MB continue to decrease with the increasing CEO content, which is suggested by the rougher surface of PLA fibers, as seen in SEM analysis. The decrease in air permeability could retard gas exchange and evaporation of water of fruit during the storage time.

ATR−FTIR Analysis. Figure 4 shows ATR−FTIR spectra of PLA MB, the modified PLA MB, CS@PLA MB, and CEO/CS@PLA MB with different CEO contents. In the ATR−FTIR spectrogram of PLA MB, the characteristic peaks at 2995 and 2944 cm^{-1} are the symmetrical stretching vibration peak of $-CH_3$ and the asymmetrical stretching vibration peak of C−H, respectively. The peak at 1750 cm^{-1} is the stretching vibration peak of −C═O. The peaks at 1450 and 1357 cm^{-1} reflect the symmetric and asymmetric bending vibration peaks of C−H in $-CH_3$, respectively.

https://doi.org/10.1021/acsomega.3c06024
ACS Omega 2023, 8, 42907−42920

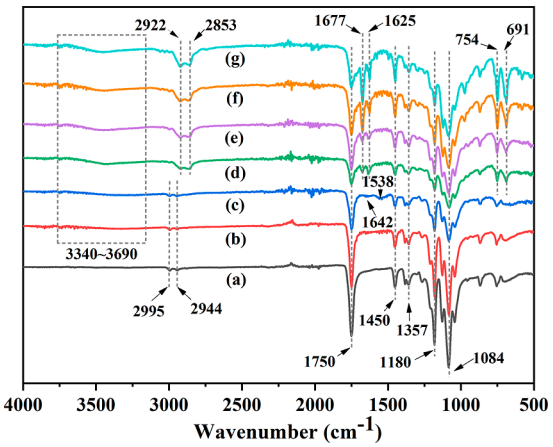

Figure 4. ATR−FTIR spectra of PLA MB, the modified PLA MB, CS@PLA MB, and CEO/CS@PLA MB with different CEO contents: (a) PLA MB, (b) the modified PLA MB, (c) CS@PLA MB, (d) $CEO_{0.5}$/CS@PLA MB, (e) CEO_1/CS@PLA MB, (f) $CEO_{1.5}$/CS@PLA MB, and (g) CEO_2/CS@PLA MB.

Moreover, the peaks at 1084 and 1180 cm^{-1} correspond to the symmetric and asymmetric stretching vibration peaks of −C−O−C−. These infrared characteristic peaks of PLA are in agreement with the reported literature[45,46] and are kept in the spectra of the other samples. The modified PLA MB spectrum shows a broad peak between 3240 and 3280 cm^{-1} corresponding to the stretching vibrations of N−H in $-NH_2$ and O−H in −OH, respectively,[47] meaning the formation of the PDA layer on the surface of PLA MB. For CS@PLA MB, the characteristic peaks of CS appear at 1642 cm^{-1} belonging to C−O (amido bond I) and 1538 cm^{-1} belonging to N−H (amido bond II).[48] In the spectra of CEO/CS@PLA MB with different CEO contents, the peaks at 2926 and 2853 cm^{-1} reflect the stretching vibration of the C−H and $-CH_2$ in CEO.[49,50] The peaks at 1677 and 1625 cm^{-1} correspond to the stretching vibration of C═O and C−C of CIN in CEO, respectively. Moreover, the obvious peaks at 754 and 691 cm^{-1} are attributed to the stretching vibration of benzene ring and C−H in olefin of CEO.[51,52] With the increasing of the CEO content, the characteristic peaks belonging to CEO strengthen. These phenomena prove that both CS and CEO have been loaded on the surface of PLA MB. It is attributed to the formation of a hydrogen bond between −OH groups of PDA and CS, and the condensation reaction of the aldehyde group (−CHO) of CIN in CEO with −OH of PDA.

Loading Ratio Analysis. The loading ratios of CEO/CS@PLA MB with different CEO contents are listed in Table 1 to quantify the reaction of CEO/CS solution with the modified PLA MB during the fabrication of CEO/CS@PLA MB. The loading ratio of $CEO_{0.5}$/CS@PLA MB is about 15.66%. When the CEO content increases, the loading ratio of CEO/CS@PLA MB is promoted. It is explained that the increasing −CHO in CEO is involved in the reaction with −OH of PDA.

XRD Analysis. Figure 5a shows the XRD patterns of PLA MB, the modified PLA MB, CS@PLA MB, and CEO/CS@PLA MB with different CEO contents. In the PLA MB pattern, there exist a diffraction peak at around 16.85°, corresponding to the (110)/(200) crystal plane of PLA α crystal.[53] After being modified by PDA, this characteristic diffraction peak is retained. In the CS@PLA MB pattern, the characteristic diffraction peaks of CS appear at 14.98, 19.22, and 22.57°, corresponding to (120), (102), and (122) crystal planes (PDF #39-1894). Additionally, the diffraction peak at 16.97° corresponding to the (002) crystal plane of CS coincides with that of PLA, which obviously strengthens the intensity of the diffraction peak at 16.85°. For CEO/CS@PLA MB, the intensity of the peak at 16.85° is weakened. The crystallinity (X_c) of PLA MB, the modified PLA MB, CS@PLA MB, and CEO/CS@PLA MB with different CEO contents are obtained by use of Jade 6.5 software and plotted in Figure 5b. X_c of CS@PLA MB is obviously higher than that of PLA MB, indicating a good crystallization capacity of CS. However, the input of CEO leads to a decrease in X_c of CEO/CS@PLA MB, suggesting that CEO dilutes PLA and CS molecular chain.[54,55]

WCA Analysis. WCA of PLA MB, the modified PLA MB, CS@PLA MB, and CEO/CS@PLA MB with different CEO contents is shown in Figure 6. WCA of PLA MB is about 126.79°, showing the apparent hydrophobicity. The WCA of the modified PLA MB distinctly reduces to 51.36°, indicting the successful transformation of the PLA MB surface from hydrophobicity to hydrophilia. The reason is that the hydrophilic −OH and $-NH_2$ of PDA have been on the surface of PLA, as shown in the ATR−FTIR analysis. However, the WCA of both CS@PLA MB and CEO/CS@PLA MB enhances. When the CEO content increases, the WCA of CEO/CS@PLA MB keeps on increasing. The increasing roughness of the surface of the CS@PLA MB and CEO/CS@PLA MB increases their hydrophobicity. On the other hand, the increasing content of hydrophobic CEO also may lead to the enhancement of WCA.

Mechanical Properties. Figure 7 shows the stress−strain curves of PLA MB, the modified PLA MB, CS@PLA MB, and CEO/CS@PLA MB with different CEO contents. Some tensile property parameters are listed in Table 2. The tensile strength and elongation at the break of PLA MB are 0.70 MPa and 2.72% (Table 2), respectively. After the hydrophilic modification of PDA, the tensile strength and elongation at break of the modified PLA MB slightly increase. After CS is loaded, the tensile strength of CS@PLA MB obviously increases, which is explained by the formation of adhesion between the PLA fibers (Figure 1), resulting in the enhanced interaction force between PLA fibers. Additionally, an increase in X_c of CS@PLA MB is also responsible for the improvement of tensile strength (Figure 5b). After CS and CEO are simultaneously immobilized on the surface of the modified PLA MB, the tensile strength of CEO/CS@PLA MB has a decline with the increasing CEO content. It is suggested that CEO may diffuse into PLA fibers and dilutes the molecular chains, causing that X_c of CEO/CS@PLA MB

Table 1. Loading Ratio (%) of CEO/CS@PLA MB with Different CEO Contents

$CEO_{0.5}$/CS@PLA MB	CEO_1/CS@PLA MB	$CEO_{1.5}$/CS@PLA MB	CEO_2/CS@PLA MB
15.66% ± 0.0046	21.42% ± 0.0095	26.15% ± 0.0041	28.44% ± 0.011

https://doi.org/10.1021/acsomega.3c06024
ACS Omega 2023, 8, 42907−42920

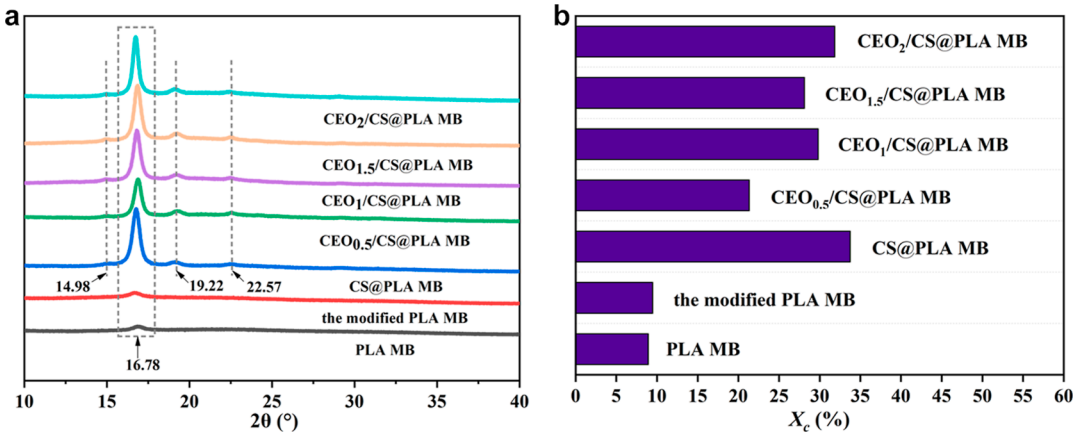

Figure 5. (a) XRD patterns and (b) crystallinity of PLA MB, the modified PLA MB, CS@PLA MB, and CEO/CS@PLA MB with different CEO contents.

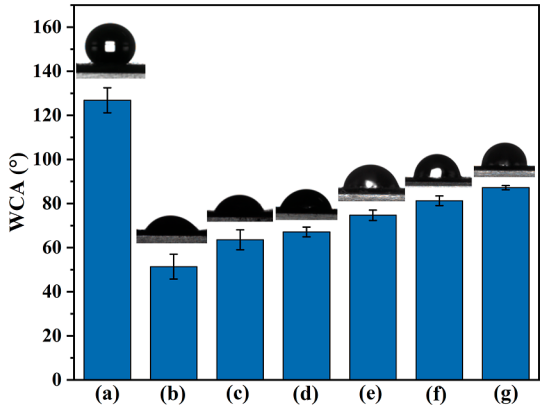

Figure 6. WCA of PLA MB, the modified PLA MB, CS@PLA MB, and CEO/CS@PLA MB with different CEO contents: (a) PLA MB, (b) the modified PLA MB, (c) CS@PLA MB, (d) $CEO_{0.5}$/CS@PLA MB, (e) CEO_1/CS@PLA MB, (f) $CEO_{1.5}$/CS@PLA MB, and (g) CEO_2/CS@PLA MB.

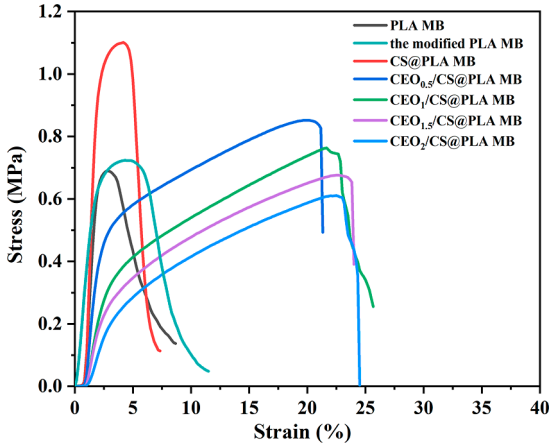

Figure 7. Stress−strain curves of PLA MB, the modified PLA MB, CS@PLA MB, and CEO/CS@PLA MB with different CEO contents.

decreases (Figure 5b) and van der Waals force of PLA molecular chains is weaken. Moreover, compared with PLA MB, the elongation at break of CEO/CS@PLA MB significantly increases, which is in agreement with the reports from Zabidi et al.[56] and Amiri et al.[57] The reason is that the dilution effect of CEO offers more free volume to the movement of PLA molecular chains and increases the flexibility of the molecular chain.

Table 2. Tensile Property Parameters of PLA MB, the Modified PLA MB, CS@PLA MB, and CEO/CS@PLA MB with Different CEO Contents

sample	tensile strength (MPa)	the elongation at break (%)
PLA MB	0.70 ± 0.03	2.72 ± 0.16
the modified PLA MB	0.78 ± 0.09	4.30 ± 0.05
CS@PLA MB	1.08 ± 0.05	5.00 ± 0.95
$CEO_{0.5}$/CS@PLA MB	0.87 ± 0.05	22.11 ± 2.88
CEO_1/CS@PLA MB	0.77 ± 0.06	23.33 ± 3.22
$CEO_{1.5}$/CS@PLA MB	0.68 ± 0.004	21.56 ± 1.13
CEO_2/CS@PLA MB	0.60 ± 0.02	21.67 ± 0.68

Antibacterial Properties. The antibacterial properties of PLA MB, CS@PLA MB, and CEO/CS@PLA MB with different CEO contents against *E. coli* and *S. aureus* were evaluated, as shown in Figure 8. Their antibacterial efficiencies are listed in Table 3. PLA MB has very low antibacterial capacity against *E. coli* and *S. aureus* (Figure 8 and Table 3). The antibacterial efficiencies of CS@PLA MB against *E. coli* and *S. aureus* are 61.49 and 67.53%, respectively. With the increasing CEO content, the antibacterial efficiencies of CEO/CS@PLA MB enhance. When the weight ratio of CS to CEO is 1:2, the antibacterial efficiencies of CEO_2/CS@PLA MB against *E. coli* and *S. aureus* reach 99.98 and 99.99%, respectively, displaying outstanding antibacterial activity. The high antibacterial activity is ascribed to the synergistic antibacterial effect of CS and CEO. The cationic nature of the quaternary ammonium moiety is responsible for the antibacterial ability of CS. However, CS is inadequate for inhibiting *E. coli* and *S. aureus* (Table 3). The incorporation of CEO strengthens the antibacterial activity of CEO/CS@PLA MB because CIN, one of the main ingredients in CEO, has better inhibitory capacity toward both *E. coli* and *S. aureus*.[58−60] The reported studies showed that CIN can inhibit the synthesis of ATP enzyme and cytoderm and destroy the cytomembrane structure to enhance antimicrobial activity against *E. coli* and *S. aureus*, which is often found in rotten food.[58] In view of the high antibacterial activity and good mechanical

https://doi.org/10.1021/acsomega.3c06024
ACS Omega 2023, 8, 42907−42920

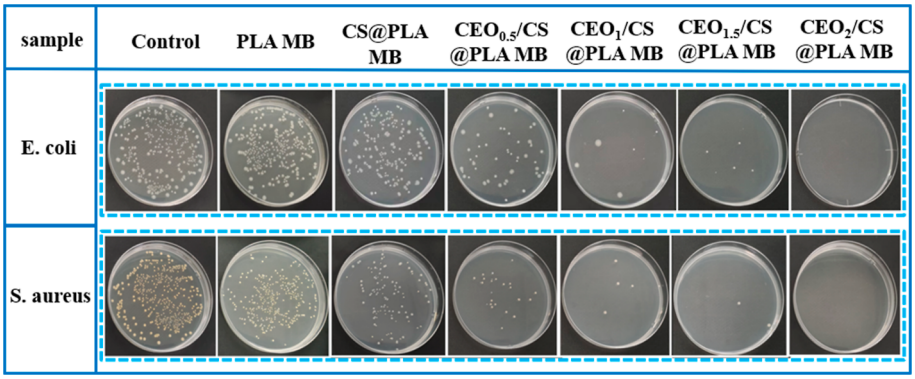

Figure 8. Change in colonies number of *E. coli* and *S. aureus* of PLA MB, CS@PLA MB, and CEO/CS@PLA MB with different CEO contents.

Table 3. Antibacterial Efficiencies (%) of PLA MB, CS@PLA MB, and CEO/CS@PLA MB with Different CEO Contents against *E. coli* and *S. aureus*

sample	E. coli	S. aureus
PLA MB	6.12 ± 1.21	4.96 ± 1.03
CS@PLA MB	61.49 ± 3.35	67.53 ± 3.53
$CEO_{0.5}$/CS@PLA MB	80.96 ± 2.20	85.98 ± 0.88
CEO_1/CS @PLA MB	98.52 ± 1.00	98.74 ± 0.36
$CEO_{1.5}$/CS@PLA MB	98.83 ± 0.12	99.17 ± 0.09
CEO_2/CS@PLA MB	99.98 ± 0.01	99.99 ± 0.01

properties, CEO_2/CS@PLA MB is selected for application in fresh strawberry preservation.

Visual Appearance. Visual appearance is an important subjective assessment for the quality of fresh fruit during their shelf life. Figure 9 shows the appearance photographs of three groups of strawberries stored at 4 ± 1 and 25 ± 3 °C, respectively. When being stored at 4 ± 1 °C, the strawberries in the control and comparative groups begin to browning and collapse on 9th days, while the strawberries in the experiment group have the similar appearance to the purchased strawberries on zeroth day. The browning of the surface of strawberries may be associated with the enzymatic browning process, in which the enzyme polyphenol oxidase oxidizes phenolic compounds in the strawberries to o-quinones, resulting in the production of brownish pigments.[61,62] The strawberries in the control and comparative groups begin to mildew on the 15th day and completely rot at the end of 18 days. However, the appearance of the strawberries in the experiment group does not visibly change until the 18th day.

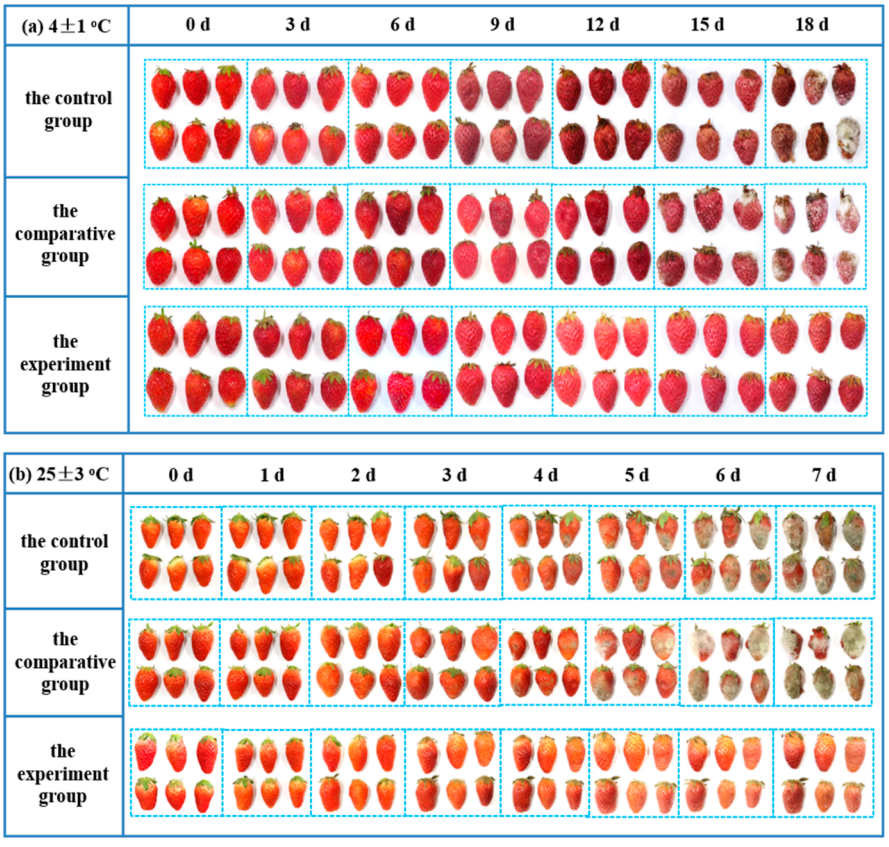

Figure 9. Visual appearance of three groups of strawberries stored at (a) 4 ± 1 and (b) 25 ± 3 °C.

https://doi.org/10.1021/acsomega.3c06024
ACS Omega 2023, 8, 42907−42920

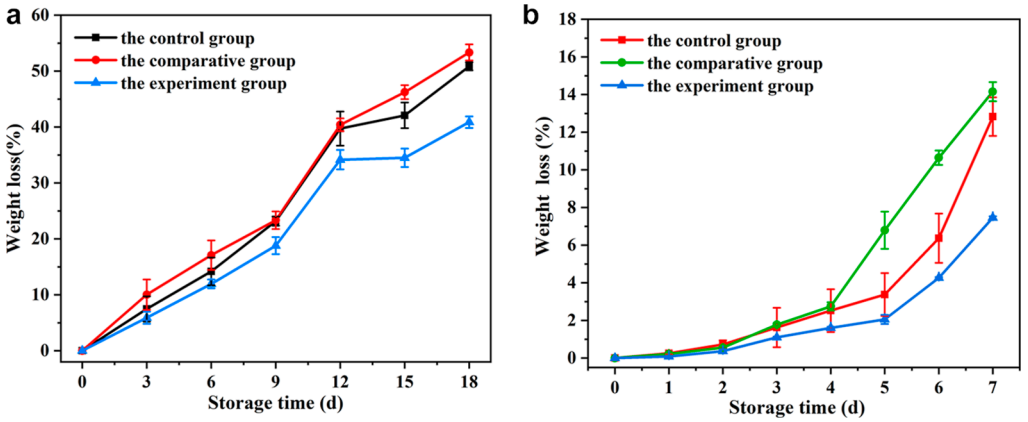

Figure 10. Weight loss of three groups of strawberries stored at (a) 4 ± 1 and (b) 25 ± 3 °C.

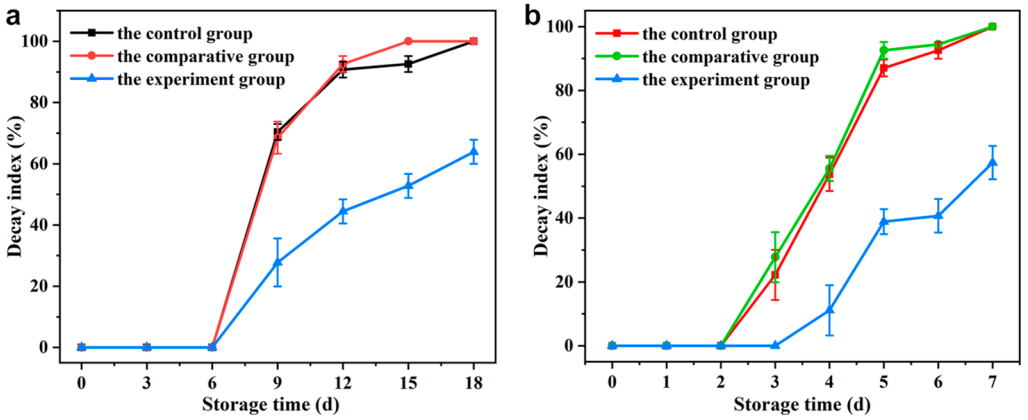

Figure 11. Decay index of three groups of strawberries stored at (a) 4 ± 1 and (b) 25 ± 3 °C.

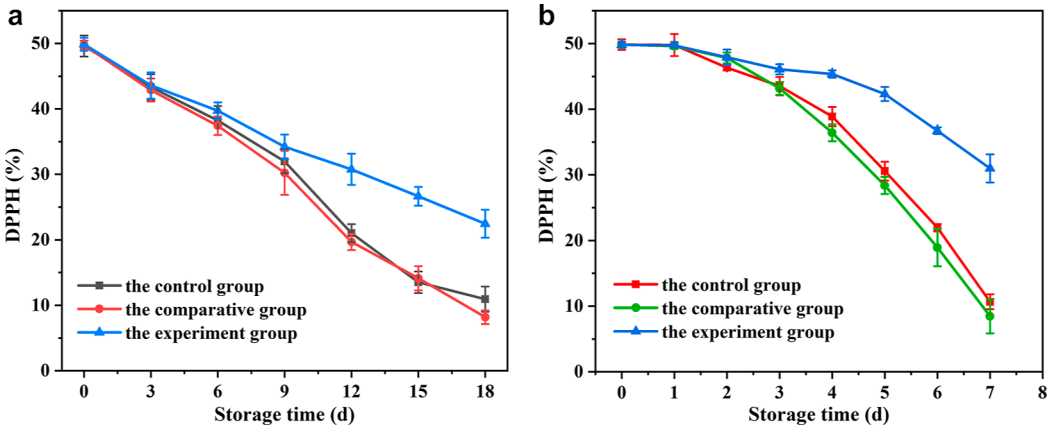

Figure 12. DPPH of three groups of strawberries stored at (a) 4 ± 1 and (b) 25 ± 3 °C.

Analogously, the strawberries in the experiment group appear to have slight browning on the 7th day at 25 ± 3 °C, while the strawberries in the control and comparative groups have completely rotten at this time. Therefore, CEO_2/CS@PLA MB can effectively maintain the appearance of strawberries.

Weight Loss. Figure 10 shows the weight loss of three groups of strawberries stored at 4 ± 1 and 25 ± 3 °C, respectively. The weight loss of three groups of strawberries keeps increasing during the storage period regardless of the storage temperature. The strawberries have a faster weight loss rate when being stored at 25 ± 3 °C. The weight loss is mainly associated with moisture evaporation through the surface of fruit and the carbon storage loss due to the respiration.[61] Compared with the other two groups, the weight loss of strawberries in the experiment is the lowest and just 7.46% at 4 ± 1 °C and 40.88% at 25 ± 3 °C, respectively. According to the research of Xin et al.,[63] the direct contact of CS with fruit may effectively reduce the weight loss of fruit. Murmu et al.[64] found that the hydrophobic CEO also could reduce moisture evaporation of fruit. Additionally, CEO_2/CS@PLA MB has the lowest gas permeability (Figure 3), which delays water loss and shrinkage of the strawberries surface.

https://doi.org/10.1021/acsomega.3c06024
ACS Omega 2023, 8, 42907−42920

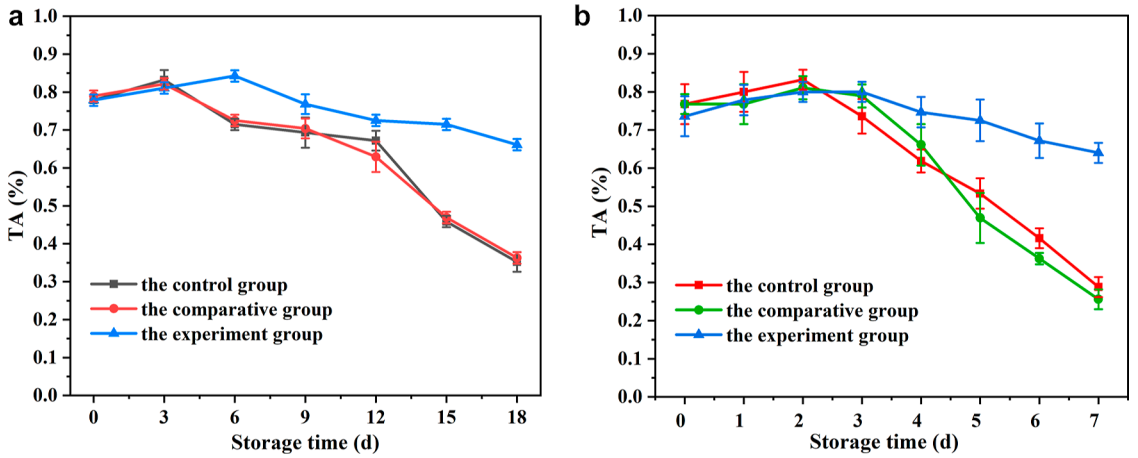

Figure 13. TA of three groups of strawberries stored at (a) 4 ± 1 and (b) 25 ± 3 °C.

Decay Index. The decay rate is the main apparent index to evaluate the storage effect of fruit. The decay index in strawberries increased during storage time for all the groups, as shown in Figure 11. In the control and comparative groups, the strawberries stored at 4 ± 1 and 25 ± 3 °C begin to rot on the 6th and 2nd days, and decay index reaches 100% on the 18th and 7th day, respectively. The application of CEO_2/CS@PLA MB has a significant positive effect on postponing strawberry spoilage during storage time. In the experiment group, the strawberries have the lowest decay rate, decay indexes are 42.59% on the 18th day at 4 ± 1 °C, and 63.89% on the 7th day at 25 ± 3 °C. According to the reported literature,[65] both CS and CEO slow down the oxygen uptake, respiration rate, and ethylene production of strawberries, which retards bacteria and fungi growth. Moreover, the volatile substances released by the CEO can interact with fungal cell membranes and influence their mobility and permeability, leading to the deterioration of conidia or mycelium.[60,66,67]

DPPH Scavenging Activity. DPPH is a stable lipid-soluble radical that discolors in the presence of antioxidant compounds and usually used to evaluate the antioxidant capacity of fruit.[67] As shown in Figure 12, DPPH scavenging activity of the strawberries decreases during the storage time but is improved when CEO_2/CS@PLA CMB is applied on preservation of the strawberries. There is no distinct difference in DPPH scavenging activity of the strawberries between the control and comparative groups. In these two groups, DPPH of the strawberries declines 38.69 and 41.56% on the 18th day at 4 ± 1 °C, respectively. However, the strawberries in the experiment group just decreases 27.40%, indicating the highest antioxidant capacity. The similar result can be observed when the strawberries are stored at 25 ± 3 °C. It is suggested that the synergistic effect of CS and CEO inhibits the biochemical reaction of strawberries, scavenges hydroxyl radicals, and reduces oxygen exchange.[68]

TA. TA is expressed in terms of the total quantity of citric acid, which is the predominant organic acid in strawberries and can reflect the quality of fruit.[69] In Figure 13, TA of the strawberries first slightly increases and then decreases regardless of the storage temperature. The slight increase in TA on the first 2 or 3 days is due to the ripening process of strawberries after harvesting, while the subsequent decrease is ascribed to the metabolism of the strawberries and consumption of organic acids during the respiratory process.[70] The strawberries stored at 4 ± 1 °C have a lower consumption rate of TA than those stored at 25± 3 °C, which reflects the slower metabolism process of the strawberries at low temperature. Moreover, TA of the strawberries in the experiment group maintains a higher level than those of the other two groups. According to Khanjari et al.[71] and Dong and Wang,[72] both CS and CEO can modify the metabolic and respiration pattern of strawberries and reduce the consumption of organic acids.

CONCLUSIONS

In this study, CEO/CS@PLA MB with high antibacterial activity was developed and applied to the preservation of fresh strawberry. PLA MB was first modified by PDA to obtain the active surface. Then, the combination of CS and CEO was loaded on the surface of the modified PLA MB via a simple one-pot method. Compared with PLA MB, the fiber surface of CEO/CS@PLA MB was rough depending on the CEO content, which caused the increase in the average diameter of PLA fibers and the decrease in the average pore diameter and air permeability. The loading ratio of the CEO/CS@PLA MB was enhanced when the CEO content increased. After being modified by PDA, the WCA of PLA MB obviously decreases. However, after CEO was added, the WCA of CEO/CS@PLA MB increased. With the increase of the CEO content, the tensile strength of CEO/CS@PLA MB had a decrease, whereas the elongation at break significantly increased. The synergistic effect of CS and CEO remarkably enhanced the antibacterial activity of the CEO/CS@PLA MB against *E. coli* and *S. aureus*. When the weight ratio of CS to CEO was 1:2, the antibacterial efficiencies of CEO_2/CS@PLA MB against *E. coli* and *S. aureus* were 99.98 and 99.99%, respectively. When being applied on the preservation of fresh strawberry, CEO_2/CS@PLA MB could effectively slow down spoilage, mildew, and weight loss of the strawberry and retard the oxidization and the consumption of TA. The application of CEO_2/CS@PLA MB has evident positive effect on extending the shelf life of the strawberry.

AUTHOR INFORMATION

Corresponding Author

Bin Yu − *College of Textiles Science and Engineering, Zhejiang Sci-Tech University, Hangzhou 310018, China; Zhejiang Provincial Innovation Center of Advanced Textile*

https://doi.org/10.1021/acsomega.3c06024
ACS Omega 2023, 8, 42907−42920

Technology, Shaoxing 312000, China; orcid.org/0000-0001-9988-7139; Email: yubin7712@163.com

Authors

Hui Sun − *College of Textiles Science and Engineering, Zhejiang Sci-Tech University, Hangzhou 310018, China; Zhejiang Provincial Innovation Center of Advanced Textile Technology, Shaoxing 312000, China;* orcid.org/0000-0001-7589-8108

Bingbing Wang − *College of Textiles Science and Engineering, Zhejiang Sci-Tech University, Hangzhou 310018, China; Zhejiang Provincial Innovation Center of Advanced Textile Technology, Shaoxing 312000, China*

Youxiu Xie − *College of Textiles Science and Engineering, Zhejiang Sci-Tech University, Hangzhou 310018, China; Zhejiang Provincial Innovation Center of Advanced Textile Technology, Shaoxing 312000, China*

Fengchun Li − *College of Textiles Science and Engineering, Zhejiang Sci-Tech University, Hangzhou 310018, China; Zhejiang Provincial Innovation Center of Advanced Textile Technology, Shaoxing 312000, China*

Tao Xu − *College of Textiles Science and Engineering, Zhejiang Sci-Tech University, Hangzhou 310018, China; Zhejiang Provincial Innovation Center of Advanced Textile Technology, Shaoxing 312000, China*

Complete contact information is available at: https://pubs.acs.org/10.1021/acsomega.3c06024

Author Contributions

Bin Yu: conceptualization, methodology, investigation, and data curation. Hui Sun: methodology, investigation, data curation, and writing. Bingbing Wang: investigation, data curation, and review. Youxiu Xie: data curation and editing. Fengchun Li: data curation and editing. Tao Xu: investigation.

Funding

This work was supported by the Natural Science Foundation of Zhejiang Province of China (no. LTGS23E030005).

Notes

The authors declare no competing financial interest.

■ ACKNOWLEDGMENTS

This work was also supported by the Zhejiang Province "High-level Talent Special Support Program" Scientific and Technological Innovation Leader project (no. 2021R52031).

■ REFERENCES

(1) Al-Adham, I. S. I.; Al-Hmoud, N. D.; Khalil, E.; Kierans, M.; Collier, P. J. Microemulsions are highly effective anti-biofilm agents. *Lett. Appl. Microbiol.* **2003**, *36*, 97−100.

(2) Falleh, H.; Ben Jemaa, M.; Saada, M.; Ksouri, R. Essential oils: A promising eco-friendly food preservative. *Food Chem.* **2020**, *330*, 127268.

(3) Torres-Giner, S.; Echegoyen, Y.; Teruel-Juanes, R.; Badia, J. D.; Ribes-Greus, A.; Lagaron, J. M. Electrospun Poly(ethylene-co-vinyl alcohol)/Graphene Nanoplatelets Composites of Interest in Intelligent Food Packaging Applications. *Nanomaterials* **2018**, *8*, 745.

(4) Ahari, H.; Soufiani, S. P. Smart and active food packaging: Insights in novel food packaging. *Front. Microbiol.* **2021**, *12*, 657233.

(5) de la Caba, K.; Guerrero, P.; Trung, T. S.; Cruz-Romero, M.; Kerry, J. P.; Fluhr, J.; Maurer, M.; Kruijssen, F.; Albalat, A.; Bunting, S.; et al. From seafood waste to active seafood packaging: An emerging opportunity of the circular economy. *J. Clean. Prod.* **2019**, *208*, 86−98.

(6) Atta, O. M.; Manan, S.; Shahzad, A.; Ul-Islam, M.; Ullah, M. W.; Yang, G. Biobased materials for active food packaging: A review. *Food Hydrocolloids* **2022**, *125*, 107419.

(7) Wang, J.; Han, X.; Zhang, C.; Liu, K.; Duan, G. Source of Nanocellulose and Its Application in Nanocomposite Packaging Material: A Review. *Nanomaterials* **2022**, *12*, 3158.

(8) Motelica, L.; Ficai, D.; Oprea, O.; Ficai, A.; Trusca, R. D.; Andronescu, E.; Holban, A. M. Biodegradable Alginate Films with ZnO Nanoparticles and Citronella Essential Oil-A Novel Antimicrobial Structure. *Pharmaceutics* **2021**, *13*, 1020.

(9) Huang, H. L.; Tsai, I. L.; Lin, C.; Hang, Y. H.; Ho, Y. C.; Tsai, M. L.; Mi, F. L. Intelligent films of marine polysaccharides and purple cauliflower extract for food packaging and spoilage monitoring. *Carbohydr. Polym.* **2023**, *299*, 120133.

(10) Lu, Y.; Luo, Q.; Chu, Y.; Tao, N.; Deng, S.; Wang, L.; Li, L. Application of Gelatin in Food Packaging: A Review. *Polymers* **2022**, *14*, 436.

(11) Tagrida, M.; Nilsuwan, K.; Gulzar, S.; Prodpran, T.; Benjakul, S. Fish gelatin/chitosan blend films incorporated with betel (Piper betle L.) leaf ethanolic extracts: Characteristics, antioxidant and antimicrobial properties. *Food Hydrocolloids* **2023**, *137*, 108316.

(12) Gürler, N.; Pekdemir, M. E.; Torğut, G.; Kök, M. Binary PCL-waste photopolymer blends for biodegradable food packaging applications. *J. Mol. Struct.* **2023**, *1279*, 134990.

(13) Phothisarattana, D.; Wongphan, P.; Promhuad, K.; Promsorn, J.; Harnkarnsujarit, N. Blown film extrusion of PBAT/TPS/ZnO nanocomposites for shelf-life extension of meat packaging. *Colloids Surf., B* **2022**, *214*, 112472.

(14) Conn, R. E.; Kolstad, J. J.; Borzelleca, J. F.; Dixler, D. S.; Filer, L.; Ladu, B.; Pariza, M. W. Safety assessment of polylactide (PLA) for use as a food-contact polymer. *Food Chem. Toxicol.* **1995**, *33*, 273−283.

(15) Kirac, F. T.; Dagdelen, A. F.; Saricaoglu, F. T. Recent advances in polylactic acid biopolymer films used in food packaging systems. *J. Food Nutr. Res.* **2022**, *61*, 1−15.

(16) Zhao, L.; Duan, G.; Zhang, G.; Yang, H.; He, S.; Jiang, S. Electrospun Functional Materials toward Food Packaging Applications: A Review. *Nanomaterials* **2020**, *10*, 150.

(17) Shao, L.; Xi, Y.; Weng, Y. Recent Advances in PLA-Based Antibacterial Food Packaging and Its Applications. *Molecules* **2022**, *27*, 5953.

(18) Han, W. H.; Li, X.; Yu, G. F.; Wang, B. C.; Huang, L. P.; Wang, J.; Long, Y. Z. Recent advances in the food application of electrospun nanofibers. *J. Ind. Eng. Chem.* **2022**, *110*, 15−26.

(19) Min, T.; Zhou, L.; Sun, X.; Du, H.; Zhu, Z.; Wen, Y. Electrospun functional polymeric nanofibers for active food packaging: A review. *Food Chem.* **2022**, *391*, 133239.

(20) Vargas Romero, E.; Lim, L. T.; Suárez Mahecha, H.; Bohrer, B. M. The Effect of Electrospun Polycaprolactone Nonwovens Containing Chitosan and Propolis Extracts on Fresh Pork Packaged in Linear Low-Density Polyethylene Films. *Foods* **2021**, *10*, 1110.

(21) Ebrahimzadeh, S.; Bari, M. R.; Hamishehkar, H.; Kafil, H. S.; Lim, L. T. Essential oils-loaded electrospun chitosan-poly(vinyl alcohol) nonwovens laminated on chitosan film as bilayer bioactive edible films. *LWT–Food Sci. Technol.* **2021**, *144*, 111217.

(22) Yu, J.; Zhao, T.; Li, C.; Pan, H.; Tan, Z.; Yang, H.; Zhang, H. Preparation and characterization of biodegradable polylactic acid/poly (butyleneadipate- co-terephthalate) melt-blown nonwovens for oil-water separation. 11 July, 2023. [Preprint]. researchsquare.com.

(23) Babapour, H.; Jalali, H.; Mohammadi Nafchi, A. The synergistic effects of zinc oxide nanoparticles and fennel essential oil on physicochemical, mechanical, and antibacterial properties of potato starch films. *Food Sci. Nutr.* **2021**, *9*, 3893−3905.

(24) Bahrami, A.; Delshadi, R.; Assadpour, E.; Jafari, S. M.; Williams, L. Antimicrobial-loaded nanocarriers for food packaging applications. *Adv. Colloid Interface Sci.* **2020**, *278*, 102140.

(25) Abd El-Hack, M. E.; El-Saadony, M. T.; Shafi, M. E.; Zabermawi, N. M.; Arif, M.; Batiha, G. E.; Khafaga, A. F.; Abd El-Hakim, Y. M.; Al-Sagheer, A. A. Antimicrobial and antioxidant

properties of chitosan and its derivatives and their applications: A review. *Int. J. Biol. Macromol.* **2020**, *164*, 2726−2744.
(26) Zhang, Y.; Dang, Q.; Liu, C.; Yan, J.; Cha, D.; Liang, S.; Li, X.; Fan, B. Synthesis, characterization, and evaluation of poly-(aminoethyl) modified chitosan and its hydrogel used as antibacterial wound dressing. *Int. J. Biol. Macromol.* **2017**, *102*, 457−467.
(27) Manzoor, A.; Dar, A. H.; Pandey, V. K.; Shams, R.; Khan, S.; Panesar, P. S.; Kennedy, J. F.; Fayaz, U.; Khan, S. A. Recent insights into polysaccharide-based hydrogels and their potential applications in food sector: A review. *Int. J. Biol. Macromol.* **2022**, *213*, 987−1006.
(28) Ruan, X.; Li, P.; Wang, C.; He, Z.; Liu, Y.; Zhou, C.; Du, L.; Song, S.; Yang, Z. Synergistic antibacterial activity of chitosan modified by double antibacterial agents as coating material for fruits preservation. *Int. J. Biol. Macromol.* **2022**, *222*, 3100−3107.
(29) Chen, S.; Zhang, Z.; Wei, X.; Sui, Z.; Geng, J.; Xiao, J.; Huang, D. Antibacterial and antioxidant water-degradable food packaging chitosan film prepared from American cockroach. *Food Biosci.* **2022**, *49*, 101893.
(30) Alshallash, K. S.; Sharaf, M.; Abdel-Aziz, H. F.; Arif, M.; Hamdy, A. E.; Khalifa, S. M.; Hassan, M. F.; Abou Ghazala, M. M.; Bondok, A.; Ibrahim, M. T. S.; et al. Postharvest physiology and biochemistry of Valencia orange after coatings with chitosan nanoparticles as edible for green mold protection under room storage conditions. *Front. Plant Sci.* **2022**, *13*, 1034535.
(31) Zhu, D.; Cheng, H.; Li, J.; Zhang, W.; Shen, Y.; Chen, S.; Ge, Z.; Chen, S. Enhanced water-solubility and antibacterial activity of novel chitosan derivatives modified with quaternary phosphonium salt. *Mater. Sci. Eng., C* **2016**, *61*, 79−84.
(32) Anitha, A.; Sowmya, S.; Kumar, P. S.; Deepthi, S.; Chennazhi, K. P.; Ehrlich, H.; Tsurkan, M.; Jayakumar, R. Chitin and chitosan in selected biomedical applications. *Prog. Polym. Sci.* **2014**, *39*, 1644−1667.
(33) Liu, Z.; Wang, L.; Zhao, X.; Luo, Y.; Zheng, K.; Wu, M. Highly effective antibacterial AgNPs@hinokitiol grafted chitosan for construction of durable antibacterial fabrics. *Int. J. Biol. Macromol.* **2022**, *209*, 963−971.
(34) Zhang, X.; Ismail, B. B.; Cheng, H.; Jin, T. Z.; Qian, M.; Arabi, S. A.; Liu, D.; Guo, M. Emerging chitosan-essential oil films and coatings for food preservation-A review of advances and applications. *Carbohydr. Polym.* **2021**, *273*, 118616.
(35) Siavash Saei-Dehkordi, S.; Fallah, A. A.; Heidari-Nasirabadi, M.; Moradi, M. Chemical composition, antioxidative capacity and interactive antimicrobial potency of Satureja khuzestanica Jamzad essential oil and antimicrobial agents against selected food-related microorganisms. *Int. J. Food Sci. Technol.* **2012**, *47*, 1579−1585.
(36) Tajkarimi, M. M.; Ibrahim, S. A.; Cliver, D. O. Antimicrobial herb and spice compounds in food. *Food Control* **2010**, *21*, 1199−1218.
(37) Siripatrawan, U. Active food packaging from chitosan incorporated with plant polyphenols. In *Novel Approaches of Nanotechnology in Food*; Grumezescu, F., Ed.; Academic Press: London, 2016; pp 465−507.
(38) Sharma, S.; Barkauskaite, S.; Jaiswal, A. K.; Jaiswal, S. Essential oils as additives in active food packaging. *Food Chem.* **2021**, *343*, 128403.
(39) Khaliq, G.; Ramzan, M.; Baloch, A. H. Effect of Aloe vera gel coating enriched with Fagonia indica plant extract on physicochemical and antioxidant activity of sapodilla fruit during postharvest storage. *Food Chem.* **2019**, *286*, 346−353.
(40) Zheng, X. L.; Tian, S. P.; Gidley, M. J.; Yue, H.; Li, B. Q.; Xu, Y.; Zhou, Z. W. Slowing the deterioration of mango fruit during cold storage by pre-storage application of oxalic acid. *J. Hortic. Sci. Biotechnol.* **2007**, *82*, 707−714.
(41) Parsa, Z.; Roozbehi, S.; Hosseinifarahi, M.; Radi, M.; Amiri, S. Integration of pomegranate peel extract (PPE) with calcium sulphate ($CaSO_4$): A friendly treatment for extending shelf-life and maintaining postharvest quality of sweet cherry fruit. *J. Food Process. Preserv.* **2021**, *45*, No. e15089.
(42) Li, N.; Xiong, X.; Ha, X.; Wei, X. Comparative preservation effect of watersoluble and insoluble chitosan from Tenebrio molitor waste. *Int. J. Biol. Macromol.* **2019**, *133*, 165−171.
(43) Huang, C.; Wang, X.; Yang, P.; Shi, S.; Duan, G.; Liu, X.; Li, Y. Size Regulation of Polydopamine Nanoparticles by Boronic Acid and Lewis Base. *Macromol. Rapid Commun.* **2023**, *44*, 2100916.
(44) Zou, Y.; Yang, P.; Yang, L.; Li, N.; Duan, G.; Liu, X.; Li, Y. Boosting solar steam generation by photothermal enhanced polydopamine/wood composites. *Polymer* **2021**, *217*, 123464.
(45) Tosakul, T.; Suetong, P.; Chanthot, P.; Pattamaprom, C. Degradation of polylactic acid and polylactic acid/natural rubber blown films in aquatic environment. *J. Polym. Res.* **2022**, *29*, 242.
(46) Li, S.; He, T.; Liao, X.; Yang, Q.; Li, G. Structural changes and crystallization kinetics of polylactide under CO_2 investigated using high-pressure Fourier transform infrared spectroscopy. *Polym. Int.* **2015**, *64*, 1762−1769.
(47) Qin, W.; Lei, K.; Yan, M.; Li, Z.; Yan, Y.; Hu, Y.; Wu, Z.; He, J.; Chen, L. Carbon fiber-reinforced epoxy composite properties improvement by incorporation of polydopamine sizing at fiber-matrix interface. *Polym. Compos.* **2023**, *44*, 2441−2448.
(48) Lee, S. J.; Gwak, M. A.; Chathuranga, K.; Lee, J. S.; Koo, J.; Park, W. H. Multifunctional chitosan/tannic acid composite films with improved anti-UV, antioxidant, and antimicrobial properties for active food packaging. *Food Hydrocolloids* **2023**, *136*, 108249.
(49) Zhou, Y.; Wu, X.; Chen, J.; He, J. Effects of cinnamon essential oil on the physical, mechanical, structural and thermal properties of cassava starch-based edible films. *Int. J. Biol. Macromol.* **2021**, *184*, 574−583.
(50) Coyotl-Pérez, W. A.; Morales-Rabanales, Q. N.; Lozoya-Gloria, E.; Becerra-Martínez, E.; Ramírez-García, S. A.; Mosso-González, C. M.; Villa-Ruano, N. Fungistatic Films Containing Cinnamon Essential Oil: New Coatings to Preserve the Nutraceutical Content of Avocado Fruit against Fusariosis. *Chem. Biodivers.* **2022**, *19*, No. e202200441.
(51) Yang, K.; Liu, A.; Hu, A.; Li, J.; Zen, Z.; Liu, Y.; Tang, S.; Li, C. Preparation and characterization of cinnamon essential oil nanocapsules and comparison of volatile components and antibacterial ability of cinnamon essential oil before and after encapsulation. *Food Control* **2021**, *123*, 107783.
(52) Bagheri, L.; Khodaei, N.; Salmieri, S.; Karboune, S.; Lacroix, M. Correlation between chemical composition and antimicrobial properties of essential oils against most common food pathogens and spoilers: In-vitro efficacy and predictive modelling. *Microb. Pathog.* **2020**, *147*, 104212.
(53) Hoogsteen, W.; Postema, A. R.; Pennings, A. J.; Ten Brinke, G.; Zugenmaier, P. Crystal structure, conformation, and morphology of solution-spun poly(L-lactide) fibers. *Macromolecules* **1990**, *23*, 634−642.
(54) Li, F.; Zhang, C.; Weng, Y. Improvement of the Gas Barrier Properties of PLA/OMMT Films by Regulating the Interlayer Spacing of OMMT and the Crystallinity of PLA. *ACS Omega* **2020**, *5*, 18675−18684.
(55) Zhang, W.; Shen, J.; Gao, P.; Jiang, Q.; Xia, W. Sustainable chitosan films containing a betaine-based deep eutectic solvent and lignin: Physicochemical, antioxidant, and antimicrobial properties. *Food Hydrocolloids* **2022**, *129*, 107656.
(56) Zabidi, N. A.; Nazri, F.; Tawakkal, I. S. M. A.; Basri, M. S. M.; Basha, R. K.; Othman, S. H. Characterization of active and pH-sensitive poly(lactic acid) (PLA)/nanofibrillated cellulose (NFC) films containing essential oils and anthocyanin for food packaging application. *Int. J. Biol. Macromol.* **2022**, *212*, 220−231.
(57) Amiri, S.; Akhavan, H. R.; Zare, N.; Radi, M. Effect of gelatin-based edible coatings incorporated with aloe vera and green tea extracts on the shelf-life of fresh-cut apple. *Ital. J. Food Sci.* **2018**, *30*, 61−74.

https://doi.org/10.1021/acsomega.3c06024
ACS Omega 2023, 8, 42907−42920

(58) Zhang, Y.; Liu, X.; Wang, Y.; Jiang, P.; Quek, S. Antibacterial activity and mechanism of cinnamon essential oil against Escherichia coli and Staphylococcus aureus. *Food Control* **2016**, *59*, 282−289.
(59) Xu, J.; Lin, Q.; Sheng, M.; Ding, T.; Li, B.; Gao, Y.; Tan, Y. Antibiofilm Effect of Cinnamaldehyde-Chitosan Nanoparticles against the Biofilm of Staphylococcus aureus. *Antibiotics* **2022**, *11*, 1403.
(60) Gadkari, R. R.; Suwalka, S.; Yogi, M. R.; Ali, W.; Das, A.; Alagirusamy, R. Green synthesis of chitosan-cinnamaldehyde cross-linked nanoparticles: Characterization and antibacterial activity. *Carbohydr. Polym.* **2019**, *226*, 115298.
(61) Constabel, C. P.; Barbehenn, R. Defensive roles of polyphenol oxidase in plants. In *Induced Plant Resistance to Herbivory*; Schaller, A., Ed.; Springer: Netherlands, 2008; pp 253−270.
(62) Queiroz, C.; Mendes Lopes, M. L.; Fialho, E.; Valente-Mesquita, V. L. Polyphenol oxidase: characteristics and mechanisms of browning control. *Food Rev. Int.* **2008**, *24*, 361−375.
(63) Xin, Y.; Chen, F.; Lai, S.; Yang, H. Influence of chitosan-based coatings on the physicochemical properties and pectin nanostructure of Chinese cherry. *Postharvest Biol. Biotechnol.* **2017**, *133*, 64−71.
(64) Murmu, S. B.; Mishra, H. N. The effect of edible coating based on Arabic gum, sodium caseinate and essential oil of cinnamon and lemon grass on guava. *Food Chem.* **2018**, *245*, 820−828.
(65) Elsabee, M. Z.; Morsi, R. E.; Fathy, M. Chitosan-Oregano Essential Oil Blends Use as Antimicrobial Packaging Material. In *Antimicrobial Food Packaging*; Barros-Velazquez, J., Ed.; Academic Press: London, 2016; pp 539−551.
(66) Chaudhari, A. K.; Singh, V. K.; Das, S.; Deepika; Singh, B. K.; Dubey, N. K. Antimicrobial, Aflatoxin B1 Inhibitory and Lipid Oxidation Suppressing Potential of Anethole-Based Chitosan Nanoemulsion as Novel Preservative for Protection of Stored Maize. *Food Bioprocess Technol.* **2020**, *13*, 1462−1477.
(67) Clemente, I.; Aznar, M.; Silva, F.; Nerín, C. Antimicrobial properties and mode of action of mustard and cinnamon essential oils and their combination against foodborne bacteria. *Innovative Food Sci. Emerging Technol.* **2016**, *36*, 26−33.
(68) Popescu, P. A.; Palade, L. M.; Nicolae, I. C.; Popa, E. E.; Mitelut, A. C.; Drăghici, M. C.; Matei, F.; Popa, M. E. Chitosan-Based Edible Coatings Containing Essential Oils to Preserve the Shelf Life and Postharvest Quality Parameters of Organic Strawberries and Apples during Cold Storage. *Foods* **2022**, *11*, 3317.
(69) Hedayati, S.; Niakousari, M. Effect of Coatings of Silver Nanoparticles and Gum Arabic on Physicochemical and Microbial Properties of Green Bell Pepper (Capsicum annuum). *J. Food Process. Preserv.* **2015**, *39*, 2001−2007.
(70) Gol, N. B.; Patel, P. R.; Rao, T. R. Improvement of quality and shelf-life of strawberries with edible coatings enriched with chitosan. *Postharvest Biol. Biotechnol.* **2013**, *85*, 185−195.
(71) Khanjari, A.; Karabagias, I. K.; Kontominas, M. G. Combined effect of N,O-carboxymethyl chitosan and oregano essential oil to extend shelf life and control Listeria monocytogenes in raw chicken meat fillets. *LWT−Food Sci. Technol.* **2013**, *53*, 94−99.
(72) Dong, F.; Wang, X. Effects of carboxymethyl cellulose incorporated with garlic essential oil composite coatings for improving quality of strawberries. *Int. J. Biol. Macromol.* **2017**, *104*, 821−826.

https://doi.org/10.1021/acsomega.3c06024
ACS Omega 2023, 8, 42907−42920